Forbidden coherent transfer observed between two realizations of quasiharmonic spin systems

S. Bertaina, G. Yue, C.-E. Dutoit, and I. Chiorescu

Forbidden coherent transfer observed between two realizations of quasi-harmonic spin systems

S. Bertaina,[1, *] G. Yue,[2] C-E Dutoit,[1] and I. Chiorescu[2, †]

[1] *Aix-Marseille Université, CNRS, IM2NP (UMR 7334), Marseille, France*
[2] *Department of Physics and The National High Magnetic Field Laboratory,*
Florida State University, Tallahassee, Florida 32310, USA
(Dated: June 12, 2017)

The multi-level system ^{55}Mn^{2+} is used to generate two pseudo-harmonic level systems, as representations of the same electronic sextuplet at different nuclear spin projections. The systems are coupled using a forbidden nuclear transition induced by the crystalline anisotropy. We demonstrate Rabi oscillations between the two representations in conditions similar to two coupled pseudo-harmonic quantum oscillators. Rabi oscillations are performed at a detuned pumping frequency which matches energy difference between electro-nuclear states of different oscillators. We measure a coupling stronger than the decoherence rate, to indicate the possibility of fast information exchange between the systems.

I. INTRODUCTION

Recent advances in single spin measurements in gated nanostructures[1] and quantum dots[2] show that spin-based materials have impact in quantum technologies. One example is constituted by multi-level spin systems which have well defined spin Hamiltonians, sufficiently large to be used as multi-qubit implementations[3] and small enough to be studied by exact numerical methods. When diluted in non-magnetic matrices, electronic spins attain large coherence times[4–6] and present the possibility to be coupled coherently to nuclear spins. In such implementations, magnetic ions (such as rare-earth elements) play an essential role[7,8] with demonstrated capability to coherently exchange information between electron spins and nuclei[9,10] as well as optical photons[11]. In the current work, we are focusing on a *3d* element, Mn, which has a very low anisotropy and thus less stringent conditions for the orientation of the external field, an important flexibility for on-chip applications.

^{55}Mn^{+2} ions diluted in a MgO matrix show electron spin resonance (ESR) transitions with $\Delta S_z = 1$ and $\Delta m_I = 0$ (S_z and m_I are projections of the electronic and nuclear $S = I = 5/2$ moments respectively) at fields separated by the hyperfine interaction in $2I + 1$ well-defined groups. However, off-diagonal couplings in the spin Hamiltonian, such as anisotropy and transverse fields terms, can activate forbidden transitions $\Delta m_I \neq 0$ and/or $\Delta S_z \neq 1$. The spectroscopy of forbidden transitions in MgO:Mn^{2+} is discussed in Refs. [12] and [13] and give important information on their transition probabilities. Large Δm_I electro-nuclear mixture can be achieved by making use of crystal and transverse fields[14] as well.

The forbidden transitions reflect a coupling between different representations of the same multi-S_z system as detailed below. Although the transfer probability between electro-nuclear states is low, the coherence properties are robust and in addition it allows maneuvering the Hamiltonian in and out of the forbidden (coupled) region. By using time-domain techniques, we can perform multi-photon and/or detuned Rabi oscillations of the electronic spin states[15,16].

Here we analyze the feasibility of combining high spin electronic and nuclear systems to demonstrate coherent exchange of information between electro-nuclear states. The measurements are done by using a two-tone technique we have recently developed[17]. We present theoretical and experimental evidence of Rabi oscillations and of a driven strong coupling regime between states belonging to different m_I. Such forbidden transitions are essential to make the entire Hilbert space available for quantum information manipulation and towards the use of long-lived nuclear spin states for storage and retrieval of quantum information.

II. RABI OSCILLATIONS OF THE ELECTRO-NUCLEAR TRANSITION.

The electro-nuclear Hamiltonian[15] of the ^{55}Mn^{2+} ions is:

$$
\begin{aligned}
\mathcal{H} =& H_{CF} + \gamma \vec{H}_0 \cdot \vec{S} - A\vec{S} \cdot \vec{I} + \gamma_N \vec{H}_0 \cdot \vec{I} \\
& + \gamma \vec{h}_{mw} \cdot \vec{S} \cos(2\pi f t).
\end{aligned}
\tag{1}
$$

The first term is the crystal field, the second is the static Zeeman interaction, the third is the hyperfine interaction the fourth is the nuclear Zeeman interaction and the last one is the dynamical Zeeman interaction caused by the microwave field. $\gamma = g\mu_B/h$ is the gyromagnetic ratio ($g = 2.0014$ the g-factor, μ_B Bohr's magneton and h Planck's constant), $\gamma_N = g_N\mu_N/h$ is the nuclear gyromagnetic ratio, $S_{x,y,z}$ are the spin projection operators, $\vec{S}$ is the total spin, $A = 244$ MHz is the hyperfine constant, h_{mw} and f represent the microwave amplitude and frequency respectively, and $\vec{H}_0$ is the static field ($\vec{H}_0 \perp \vec{h}_{mw}$). $H_{CF} = a/6[S_x^4 + S_y^4 + S_z^4 - S(S+1)(3S^2+1)/5]$

with $a = 55.7$ MHz the anisotropy constant, represents the crystal field anisotropy which generates a small anharmonicity of the otherwise equally spaced Zeeman levels $S_z = -5/2...5/2$.

The model describing the multiphoton Rabi oscillations observed in MgO:Mn^{2+} was reported in Ref. [15]. However, the electron-nuclear forbidden transitions were dropped off from the model since their probability are weak compared to the multiphoton electronic transitions. In this work, the hyperfine term of $\mathcal{H}$ is no longer neglected, leading to a full Hamiltonian $S \otimes I$ with a dimensionality of 36.

Let us consider a quantum system with 36 states $|S_z \otimes I_z\rangle$, S_z and $I_z = \{-5/2, -3/2, -1/2, 1/2, 3/2, 5/2\}$, irradiated by an electromagnetic field. The spin Hamiltonian $\mathcal{H}$ can be rewritten as:

$$\mathcal{H} = \hat{E} + \hat{V}(t) = \sum_{S_z, I_z = -5/2}^{5/2} E_{S_z, I_z} |S_z \otimes I_z\rangle\langle S_z \otimes I_z| + \hat{V}(t),$$
(2)

with E_{Sz, I_z} the static energy levels, $\hat{V}(t) = \frac{\gamma}{2} h_{mw}(\hat{S}_+ + \hat{S}_-)\cos(2\pi f t)$, S_+/S_- the raising/lowering operators. Since $H_0 \gg h_{mw}$, we use the rotating wave approximation (RWA) to make Eq. (2) to be time independent. We apply the unitary transformation $U(t) = \exp(-i2\pi f \hat{S}_z t)$ to the Hamiltonian (2)[18,19]:

$$\mathcal{H}_{RWA} = U\mathcal{H}U^\dagger + i\hbar \frac{\partial U}{\partial t} U^\dagger$$
(3)

and perform exact diagonalization of $\mathcal{H}_{RWA}$. Coherent motion of spin projection S_z is analyzed using time-dependent Schrödinger equation and its FFT can reveal multiple Rabi frequencies and beatings (see below).

Previous work[15] shows that at exactly the "compensation angle" $\theta = \theta_c$ between $\vec{H}_0$ and the crystal axis z, the anharmonic effect of the H_{CF} term is compensated for and the S_z levels are equidistant. In the present study, we chose to work at this compensation angle to reduce the level structure to simple pseudo-harmonic systems and put in evidence their coupling. Note that the applied static field ensures a Zeeman splitting of $\gamma H_0 \approx f \sim 10$ GHz, much stronger than all other interactions of Eq.(1), effectively making $\vec{H}_0$ the quantization axis.

In the RWA approximation, the resonance is shown in Fig. 1 by the probe arrow where all eigen-states collapse (for $m_I = 1/2$, the blue sextuplet). The two sextuplets are two pseudo-harmonic oscillators as different realizations of the same set $|S_z\rangle$. The dashed lines indicate the effect of a large h_{mw} on the numerically computed dressed states. Note that Fig. 1 shows the levels in RWA while Fig. 2 is a sketch showing the laboratory frame picture. The assignment of spin projections S_z in Fig. 1 correlates to the slopes of the quasi-energies dependence on detuning. In Fig. 2, the two electro-nuclear transitions appear in diagonal (see the levels connected by F_+ and
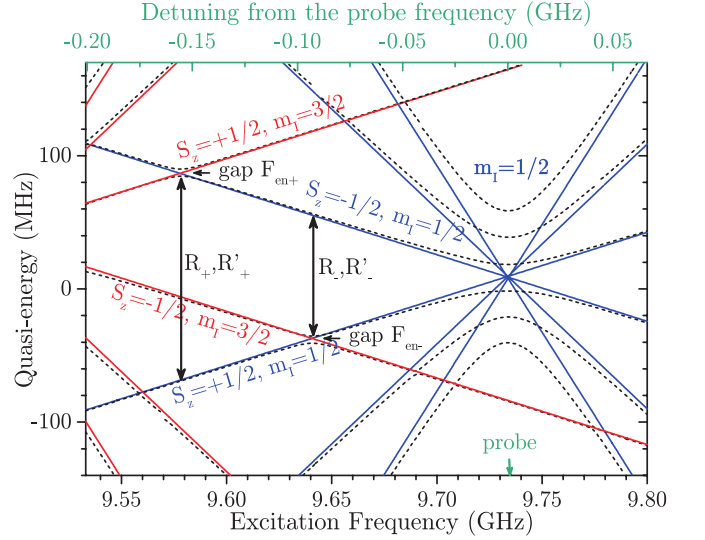

Figure 1. (color online) Quasi-energies of H in the rotating wave approximation for low (lines) and high (dashed lines) microwave power for two sextuplets S_z: $m_I = 1/2$ (blue, right) and $3/2$ (red, left). The static field corresponds to the resonance frequency (shown by the green arrow) where the equally spaced levels collapse (for $h \to 0$). Detuned Rabi oscillations, e.g. $R_\pm$ with location shown by the double-headed arrows, can be measured for any frequency in this range.
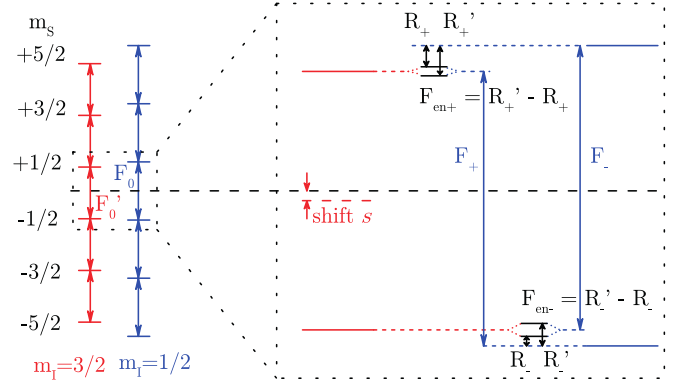

Figure 2. (color online) Sketch of H eigen-states for $m_I = 1/2$ and $3/2$. The central four states are magnified, showing the relationships $F_0 = F_- + R_- = F_+ + R_+ = F_0' + A$, as well as a splitting $F_{en\pm}$ of Rabi frequencies. The shift s (see text) enforces $R_+ \neq R_-$ and thus distinct double-headed arrows in Fig. 1.

F_- respectively), rather than as avoided level crossings as in Fig. 1.

The nature and magnitude of the forbidden transition probabilities have been studied theoretically in this system[13] and they follow (here $\theta = \theta_c = 31°$):

$$F_{en\pm} \propto 5\sin 4\theta(ah_{mw}/f)[I(I+1) - m_I(m_I - 1)].$$
(4)

Thus, the small anisotropy a is the essential ingredient to the coupling between the two oscillators, by enabling forbidden electronic transitions with $\Delta S_z = \Delta m_I = 1$.

Notable is the dependence of $F_{en\pm}$ on microwave field h_{mw} which allows *in-situ* control over the strength of coupling between the two pseudo-harmonic oscillators.

The experimental data discussed below, suggest that the dynamics of the group of four states shown in Fig. 2 can be driven independently from the other levels. This leads to a description in terms of an effective 4×4 RFA Hamiltonian:

$$H_{RF} = \Delta s_z - A s_z i_z - s i_z + 2F_{en}s_x i_x + \gamma h_{mw}s_x \quad (5)$$

where $F_{en} = F_{en\pm}$, $s_{x,z}$ and $i_{x,z}$ are the Pauli matrices for the electronic and nuclear spin operator in this effective representation and $\Delta = f - (F_0 - A/2)$ is the detuning of the pump pulse by respect to $F_0 - A/2$. The coupled oscillations take place at $\Delta, A, s, F_{en} \gg \gamma h_{mw}$ in which case analytical diagonalization of H_{RF} for $h_{mw} \sim 0$ leads to two pairs of levels:

$$S_\pm^{(1)} = A/4 \pm \frac{1}{2}\sqrt{(\Delta + s)^2 + F_{en}^2}$$
$$S_\pm^{(2)} = -A/4 \pm \frac{1}{2}\sqrt{(\Delta - s)^2 + F_{en}^2}, \quad (6)$$

with F_{en} given by Eq. 4. The splitting of each pair at $\Delta = \pm s$ is F_{en}, as expected.

Different from the strong coupling regime in cavity QED experiments[20–22] is the fact that here the Vaccum Rabi Splitting is observed under a sufficiently strong drive, since $F_{en\pm} \propto h_{mw}$. Resonant photons of energy hF_- (or hF_+) match the difference between $|0,e\rangle$ and $|1,g\rangle$, where 0 and 1 label the state of the pseudo-harmonic electronic spin system (operator s_z) and e, g label the nuclear state (operator i_z). The analogy could be further extend by taking into consideration the multi-level structure of each m_I subset, with $S_z = -5/2 \ldots 5/2$. The F_{en} transition allows the exchange of information between subsets, to be followed by spin manipulation within a subset[15,16].

III. EXPERIMENTAL PROCEDURE

Measurements were performed using a conventional Bruker Elexsys 680 pulse spectrometer. The second frequency source is provided by the ELDOR bridge of the spectrometer. The experiments are performed in a static field corresponding to $F_0 = 9.734$ GHz, $F_- = 9.641$ GHz and $F_+ = 9.586$ GHz. In fixed static field, a first ESR pulse excites the system at any frequency detuning and a second pulse reads the difference in level population at the main resonance. As explained below, this method allows us to detune two representations of multi-level systems until they are brought in resonance, to demonstrate the strong coupling regime and a coherent transfer of information between the two systems. The temperature was set to 50 K to have the relaxation time T_1 long enough to perform the pulse sequence.

A first microwave pump pulse of frequency $f = F_\pm$ drives Rabi oscillations of the Mn^{2+} spins. In order to
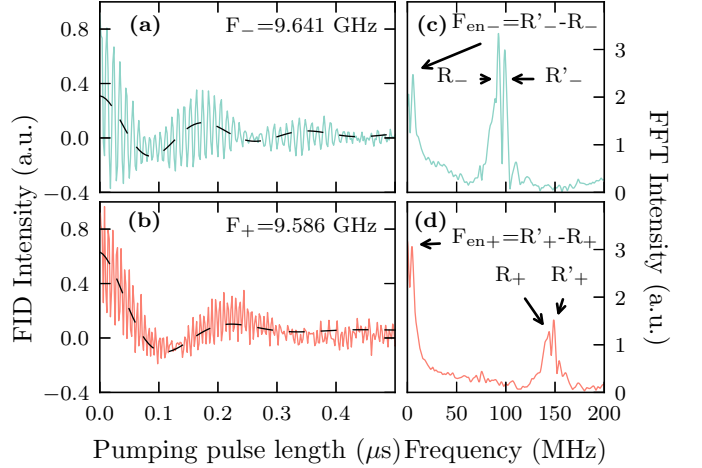

Figure 3. (color online) Rabi oscillations (left panel) for pump frequencies $F_\pm$ matching forbidden resonance conditions between two pseudo-harmonic level systems (see Fig. 2). The dashed line is a beating between two Rabi frequencies, demonstrating a coupling between the two systems stronger than the Rabi decay time. Corresponding FFT spectra are shown in the left panel, with visible strong coupling splittings $F_{en\pm} = R'_\pm - R_\pm$.

induce the coherent manipulation of an electro-nuclear forbidden transition, we set the microwave power to the maximum value available on the spectrometer. Because of the presence of a resonant cavity the amplitude of the microwave field depends on the frequency and the cavity transfer function. The h_{mw} calibration has been done using the following procedure: we measured at maximum microwave power the nutation frequency of a $S = 1/2$ calibration standard (DPPH) by sweeping the microwave frequency f and the static field H_0 to keep them in resonant condition. Using the relation between nutation frequency and microwave field: $g\mu_B h_{mw}(f)/2 = h\Omega_R(f)$ we found the microwave field amplitude as a function of the microwave frequency used for the pumping pulse. In particular we found for $f = F_0$, $h_{mw} \sim 20$ G, for $f = F_-$, $h_{mw} \sim 13$ G and for $f = F_+$, $h_{mw} \sim 10$ G.

After a time longer than the Rabi decay time but much shorter than the relaxation time T_1, a second pulse ($\pi/2$ in 20 ns) at $f = F_0$ probes the S_z component, using the intensity of the Free Induction Decay (FID) signal. The second pulse does not require a high power since it probes an allowed transition[17] $m_s = -1/2 \rightarrow 1/2$. The sample is a $(2 \times 2 \times 1)$ mm^3 single crystal of MgO doped with Mn^{2+} in a small concentration of $\sim 10^{-5}$; the crystal is oriented such that the allowed transitions appear at the same field (see the "compensation angle" θ_c above).

For clarity, only the case of $m_I = 3/2$ and $1/2$ is presented here. The sextuplets are sketched in Fig. 2 together with a magnified representation of the main ESR transition, between states $S_Z = \pm 1/2$. The Zeeman splittings are $F_0 = f$ and $F'_0 = F_0 - A$ for $m_I = 1/2$ and $3/2$ respectively. The two transitions are shifted

by an amount s which is evaluated by Drumheller[23] as a second order perturbation in A and generates the vertical shift between sextuplets in Fig. 1. The shift $s \approx 33$ MHz is in good agreement with the theoretical estimation[23] of ~ 44 MHz. Consequently, forbidden couplings between sextuplets occur at different frequencies $F_\pm = F_0 - A/2 \mp s$, allowing their individual excitation by an adequate detuning of the drive frequency f. The frequency of Rabi oscillations is shown by double headed arrows $R_\pm = F_0 - F_\pm = A/2 \pm s$. As highly detuned Rabi oscillations, their frequency depends almost linearly on the detuning from probe frequency F_0.

Moreover, if the electro-nuclear coupling between the two sextuplets is larger than the decoherence rate, a splitting of the Rabi frequencies should be observed ($F_{en\pm} = R'_\pm - R_\pm$) as illustrated in Fig. 2 and numerically calculated in Fig. 1.

IV. RESULTS AND DISCUSSIONS

Experimental results are presented in Fig. 3 as time-domain Rabi oscillations (left panel) and their Fast Fourier Transform (FFT) spectra (right panel). One observes that the Rabi frequencies are relatively large for a spin system, with $R_- \approx 100$ MHz and $R_+ \approx 150$ MHz, although they are in a detuned regime (the Rabi frequency at resonance is ≈ 34 MHz). More importantly, the coupling between the two electronic systems is sufficiently strong to overpass the Rabi decay rate of $\Gamma_R \sim 1/(250 \text{ ns})$. This leads to normal mode splitting of the two Rabi frequencies by an amount $F_{en\pm} = R'_\pm - R_\pm = 4.5$ MHz and 5.7 MHz, respectively. In the left panel of Fig. 3, the dashed line shows the F_{en+} and F_{en-} beatings with a damping of ~ 200 ns and ~ 250 ns respectively.

The two-tone technique allows the study of coupled Rabi oscillations for any detuning, in the vicinity of $F_\pm$. FFT spectra are shown in Fig. 4, as a function of drive frequency around the resonances F_+ (a) and F_- (b). The symbols represent the values of $R_\pm, R'_\pm$ (triangles) and F_{en} (circles) as FFT peaks of measured Rabi dynamics while the contour plot is calculated by exact diagonalization of H in the rotating frame. The simulations are resolving for the value of the Rabi peaks and less for their intensities, color coded from blue to dark red (arbitrary units) in Fig. 4. One notes how the Rabi oscillation accelerates with the detuning to large values, close to 200 MHz. The low frequency beating F_{en} is equal to the splitting of the two Rabi frequencies, when the resonance condition described above (Figs. 1,2) is met. Moreover, one observes an increase of the beat frequency due to detuning, similar to the coherent motion of a two-level system (TLS) driven out of resonance. Here, $F_{en\pm}$ represent the coherent motion between two pseudo-harmonic oscillators.

The height of a FFT peak in Fig. 4 represents the amplitude of the corresponding Rabi oscillation. They are extracted and shown in Fig. 5 as a function of detun-
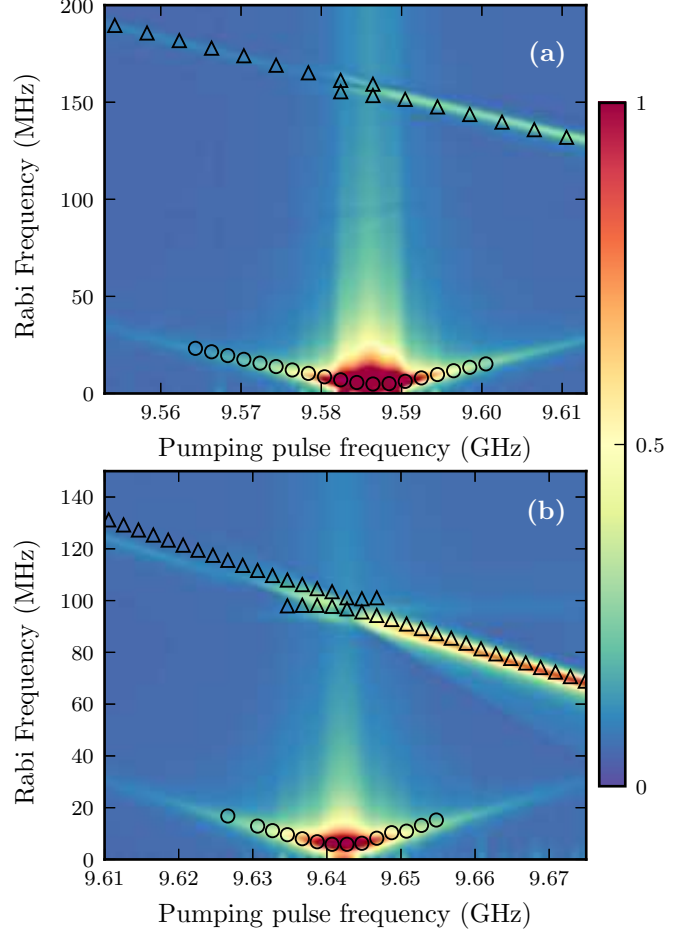

Figure 4. (color online) FFT spectra as a function of drive frequency around F_+ (a) and F_- (b). The peaks location, intensity and width indicate Rabi oscillations frequency, amplitude and decay rate. The contour plot represents FFT of simulated Rabi oscillations (the color coded scale is in arbitrary units). The symbols are FFT peaks of measured Rabi oscillations: $\triangle$ / $\circ$ correspond to the high / low frequency Rabi oscillations shown in Fig. 3

ing away from F_0. While Rabi frequency increase with detuning, the oscillation's amplitude decreases. For a TLS, the amplitude P of the Rabi frequency $F_R(\delta)$ as a function of detuning δ is described by the well-known relation[24]:

$$P = a_1 \frac{F_R(0)^2}{F_R(0)^2 + \delta^2} + a_0 \qquad (7)$$

with $a_{i=0,1} = i$ in the Rabi model, corresponding to a full swing spin-up $\leftrightarrow$ spin-down at resonance, while here they are fit parameters. The detuning δ is defined as the difference between the pump frequency f and the resonance frequency of the considered TLS: $F_\pm$ for the electro-nuclear transitions and F_0 for the spin transition.

The three situations are fitted very well by Eq. 7, as shown by dashed curves in Fig. 5. The TLS model de-
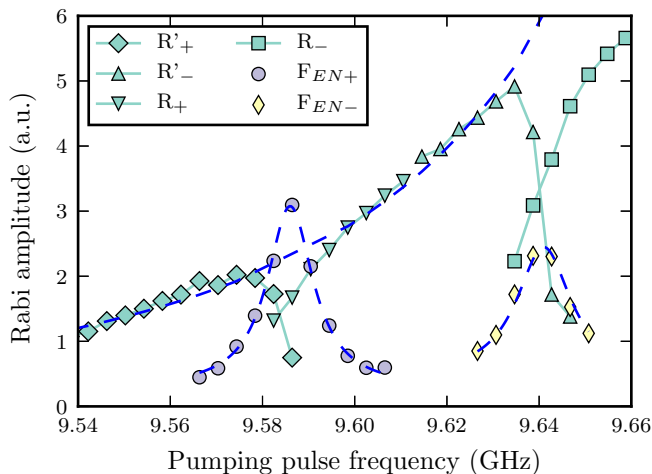
Figure 5. (color online) Amplitudes of Rabi oscillations (FFT peak intensities from Fig. 4) as a function of drive frequency, fitted by a TLS model (7) (dotted and dashed lines). In the strong coupling region, $F_{en\pm}$ are very well described by the fit.

and detuned at $F_{\pm}$ with $F_+ < F_- < F_0$. Consequently, the microwave fields at $F_{\pm}$ follow $h_{mw+} < h_{mw-}$ which leads to $F_{en+} < F_{en-}$. This case can be described by Hamiltonian (5) by replacing the term $2F_{en}s_xi_x$ with $F_{en-}(s_+i_- + s_-i_+)/2 + F_{en+}(s_+i_+ + s_-i_-)/2$.

In this case, the condition to tune the systems into the strong coupling regime, is to have $h_{mw\pm}$ sufficiently large such that $F_{en\pm} > \Gamma_R$ (defined above), condition indeed fulfilled in our experiment. The decay rate of individual (or coupled) oscillations is mostly due to the inhomogeneity of the microwave field[25,26]. Volume integration over the entire spin population, causes a fast Γ_R although the echo-detected coherence times are 1-2 orders of magnitude larger. To detect faster or larger coupled forbidden oscillations in the system presented here, one can in principle utilize setups providing larger power or sensitivity allowing the study of samples with smaller volume (and thus smaller h_{mw} inhomogeneity) or lower Mn doping concentrations (and thus lower level of long-range dipolar interactions)..

V. CONCLUSION

We show coherent transfer of state population between two equidistant level systems, $|S_z, m_I = 1/2\rangle$ and $|S_z, m_I = 3/2\rangle$ by using forbidden nuclear transitions with $\Delta m_I = 1$. The coupling between systems is tunable and is stronger than the decay rate, leading to an observable splitting of the Rabi mode and a state transfer faster than the decay time. The results open the way of combining the electronic and long-lived nuclear degrees of freedom in this multi-level system.

scribes the $R_\pm$ and $R'_\pm$ data (dotted curve, $a_1 \approx 62$ and $a_0 \approx 0$) in regions where the dynamics $R_\pm$ is not affected by the strong coupling of the two level systems. The fitted half-width at half-maximum (HWHM) gives a Rabi frequency at resonance of 31 MHz, close to a measured value of 34 MHz and in agreement with the amount of power estimated in the cavity.

In the coupled region $f \sim F_\pm$, the extracted HWHM also gives very good estimations of the beat frequencies: $F_{en+} = 6.06$ MHz and $F_{en-} = 7.2$ MHz. The other fit parameters are $a_1 = 2.8$ and 2, $a_0 = 0.27$ and 0.44, for F_+ and F_- respectively.

Since the TLS model (7) applies well to the forbidden transitions, the dynamics shown in Fig. 2 can be described by the effective Hamiltonian given in Sect. II. Following Eq. 4, the couplings $F_{en\pm}$ should be equal while in our experiment they are slightly different. This is due to the cavity resonance profile, centered around $\sim F_0$

* sylvain.bertaina@im2np.fr

† ic@magnet.fsu.edu

[1] J. T. Muhonen, J. P. Dehollain, A. Laucht, F. E. Hudson, R. Kalra, T. Sekiguchi, K. M. Itoh, D. N. Jamieson, J. C. McCallum, A. S. Dzurak, et al., *Storing quantum information for 30 seconds in a nanoelectronic device*, Nat. Nanotechnol. **9**, 986 (2014).

[2] M. Goryca, M. Koperski, P. Wojnar, T. Smoleński, T. Kazimierczuk, A. Golnik, and P. Kossacki, *Coherent Precession of an Individual 5/2 Spin*, Phys. Rev. Lett. **113**, 227202 (2014).

[3] M. N. Leuenberger and D. Loss, *Quantum computing in molecular magnets*, Nature **410**, 789 (2001).

[4] S. Nellutla, K. Y. Choi, M. Pati, J. van Tol, I. Chiorescu, and N. S. Dalal, *Coherent manipulation of electron spins up to ambient temperatures in $Cr^5+(S=1/2)$ doped K_3NbO_8*, Phys. Rev. Lett. **99**, (2007).

[5] S. Bertaina, S. Gambarelli, A. Tkachuk, I. N. Kurkin, B. Malkin, A. Stepanov, and B. Barbara, *Rare-earth solid-state qubits*, Nat. Nanotechnol. **2**, 39 (2007).

[6] S. Bertaina, S. Gambarelli, T. Mitra, B. Tsukerblat, A. Müller, and B. Barbara, *Quantum oscillations in a molecular magnet.*, Nature **453**, 203 (2008).

[7] S. Probst, H. Rotzinger, A. V. Ustinov, and P. A. Bushev, *Microwave multimode memory with an erbium spin ensemble*, Phys. Rev. B **92** (2015).

[8] S. Bertaina, J. H. Shim, S. Gambarelli, B. Z. Malkin, and B. Barbara, *Spin-Orbit Qubits of Rare-Earth-Metal Ions in Axially Symmetric Crystal Fields*, Phys. Rev. Lett. **103**, 226402 (2009).

[9] M. V. G. Dutt, L. Childress, L. Jiang, E. Togan, J. Maze, F. Jelezko, A. S. Zibrov, P. R. Hemmer, and M. D. Lukin, *Quantum register based on individual electronic and nuclear spin qubits in diamond*, Science **316**, 1312 (2007).

[10] G. Wolfowicz, H. Maier-Flaig, R. Marino, A. Ferrier, H. Vezin, J. J. L. Morton, and P. Goldner, *Coherent Storage of Microwave Excitations in Rare-Earth Nuclear Spins*, Phys. Rev. Lett. **114**, 170503 (2015).

[11] C. Clausen, I. Usmani, F. Bussieres, N. Sangouard, M. Afzelius, H. de Riedmatten, and N. Gisin, *Quantum storage of photonic entanglement in a crystal*, Nature **469**, 508 (2011).

[12] G. Wolga and R. Tseng, *Forbidden Transitions in the Paramagnetic-Resonance Spectrum of Mn^{2+} in Cubic MgO*, Phys. Rev. **133**, A1563 (1964).

[13] S. R. P. Smith, P. V. Auzins, and J. E. Wertz, *Angular Dependence of the Intensities of "Forbidden" Transitions of Mn2+ in MgO*, Phys. Rev. **166**, 222 (1968).

[14] M. S. Fataftah, J. M. Zadrozny, S. C. Coste, M. J. Graham, D. M. Rogers, and D. E. Freedman, *Employing forbidden transitions as qubits in a nuclear spin-free chromium complex*, J. Am. Chem. Soc. **138**, 1344 (2016).

[15] S. Bertaina, L. Chen, N. Groll, J. Van Tol, N. S. Dalal, and I. Chiorescu, *Multiphoton Coherent Manipulation in Large-Spin Qubits*, Phys. Rev. Lett. **102**, 50501 (2009).

[16] S. Bertaina, N. Groll, L. Chen, and I. Chiorescu, *Tunable multiphoton Rabi oscillations in an electronic spin system*, Phys. Rev. B **84**, 134433 (2011).

[17] S. Bertaina, M. Martens, M. Egels, D. Barakel, and I. Chiorescu, *Resonant single-photon and multiphoton coherent transitions in a detuned regime*, Phys. Rev. B **92**, 24408 (2015).

[18] C. Hicke and M. I. Dykman, *Multiphoton antiresonance in large-spin systems*, Phys. Rev. B **76**, (2007).

[19] M. N. Leuenberger and D. Loss, *Grover algorithm for large nuclear spins in semiconductors*, Phys. Rev. B **68**, 165317 (2003).

[20] I. Chiorescu, N. Groll, S. Bertaina, T. Mori, and S. Miyashita, *Magnetic strong coupling in a spin-photon system and transition to classical regime*, Phys. Rev. B **82**, 24413 (2010).

[21] Y. Kubo, F. R. Ong, P. Bertet, D. Vion, V. Jacques, D. Zheng, A. Dreau, J. F. Roch, A. Auffeves, F. Jelezko, et al., *Strong Coupling of a Spin Ensemble to a Superconducting Resonator*, Phys. Rev. Lett. **105** (2010).

[22] D. I. Schuster, A. P. Sears, E. Ginossar, L. DiCarlo, L. Frunzio, J. J. L. Morton, H. Wu, G. A. D. Briggs, B. B. Buckley, D. D. Awschalom, et al., *High-Cooperativity Coupling of Electron-Spin Ensembles to Superconducting Cavities*, Phys. Rev. Lett. **105** (2010).

[23] J. E. Drumheller and R. S. Rubins, *"Forbidden" Hyperfine Transitions in the Electron Paramagnetic Resonance of Mn^{2+} in Cubic MgO*, Phys. Rev. **133**, A1099 (1964).

[24] C. Cohen-Tannoudji, B. Diu, and F. Laloë, *Quantum Mechanics Vol.2* (John Wiley & Sons, Inc., New York, 2006).

[25] H. De Raedt, B. Barbara, S. Miyashita, K. Michielsen, S. Bertaina, and S. Gambarelli, *Quantum simulations and experiments on Rabi oscillations of spin qubits: Intrinsic vs extrinsic damping*, Phys. Rev. B **85**, 014408 (2012).

[26] E. Baibekov, I. Kurkin, M. Gafurov, B. Endeward, R. Rakhmatullin, and G. Mamin, *Coherence times and rabi oscillations in $CaWO_4$:Cr^{5+} crystal*, J. Magn. Reson. **209**, 61 (2011).